Structure and Dynamics of Binary Clusters

A. S. Clarke,[1] R. Kapral,[2] B. Moore,[3] G. Patey,[1] and X.-G. Wu[2]
[1] *Department of Chemistry, University of British Columbia, Vancouver, British Columbia, Canada V6T 1Z1*
[2] *Chemical Physics Theory Group, Department of Chemistry, University of Toronto, Toronto, Canada M5S 1A1*
[3] *Department of Chemistry, Eastern Washington University, Cheney, Washington 99004*
(Received 28 January 1993)

Phase separation dynamics and structural properties of binary liquid clusters with linear dimensions in the nanometer range are investigated. The demixing process proceeds through incipient domain formation and coarsening processes. Strong density correlations are shown to exist within the resulting phase-separated clusters. The results of this study show that cluster binary mixtures display interesting two-phase phenomena which differ from their bulk-phase analogs.

PACS numbers: 64.70.–p, 36.40.+d, 64.75.+g, 82.20.Wt

The small-system analog of the solid-liquid phase transformation process has been extensively investigated in atomic clusters [1–5]. Studies of such clusters with linear dimensions in the nanometer range (nanoclusters) have addressed questions related to the smooth character of the transition in the cluster environment and the passage to a discontinuous transition in the bulk, as well as the applicability of finite-size scaling arguments [6] and finite-size thermodynamics [7] to cluster phase transition processes.

In this Letter we consider the structural properties and phase separation dynamics of binary liquid nanoclusters. As for one-component clusters, on this length scale the free surface of the cluster gives rise to forces which influence the structure and dynamics. Our interest is in the demixing process. In this case the interface between the coexisting phases must also be taken into account. We show that while the phase separation process is different from that in the bulk there are a number of features that presage important elements in the bulk process. The existence of the interface between the two coexisting phases in the phase-separated cluster along with the presence of free surfaces give rise to distinctive structural correlations. Below we show that both static and dynamic binary mixture properties display interesting features for clusters, which distinguish this state of matter from bulk binary fluids.

We consider a simple model system consisting of two mechanically identical argonlike Lennard-Jones (LJ) species labeled A and B. The species have the same LJ parameters, $\epsilon/k_B = \epsilon_{\beta\beta}/k_B = 121$ K, $\sigma = \sigma_{\beta\beta} = 3.4$ Å, and mass $m = m_\beta = 40$ amu, for $\beta = A, B$. The cross interactions also have $\sigma = 3.4$ Å but ϵ_{AB} is varied to explore the phase separation dynamics. The relative strength of the cross interactions is gauged by the ratio $\alpha = \epsilon_{AB}/\epsilon$, which is taken to be less than unity to favor demixing. All of the studies presented below are restricted to symmetric clusters composed of a 50:50 mixture of N atoms, where $N = N_A + N_B$. Effects due to composition variations are interesting to study but will not be considered here.

Equilibrium structure.—The studies of static structural properties were carried out using constant temperature Monte Carlo (MC) simulation as well as both constant energy and constant temperature [8] molecular dynamics (MD). Starting from a regular configuration with species labels assigned randomly to the particle positions, a cluster with a given total particle number N and $\alpha = 1$ was first equilibrated at constant T using either MC or MD. Following this initial equilibration stage, α was decreased and the system was again equilibrated using MC or MD. If particle evaporation occurred, that realization of the binary cluster was discarded. The structural properties of the mixed clusters were studied as a function of α. Both magic and nonmagic number values of N_A were considered [4]. Of course, the phase-separated states of the binary clusters are metastable rather than true equilibrium states since eventually the clusters will evaporate; however, the metastable states persist for long periods of time without evaporation and can be well characterized. The transition from solidlike to liquidlike behavior generally occurs over a (cluster size-dependent) range of temperatures [1–5]. We focus on the behavior of clusters with liquidlike structures [9]. The liquidlike character was inferred from measurements of the diffusivity of the particles comprising the clusters. These measurements show, for example, that the melting temperature range is roughly 0.25 ± 0.02, 0.31 ± 0.02, 0.33 ± 0.02, and 0.36 ± 0.02 for pure clusters with $N = 25$, 76, 110, and 240, respectively. (The temperature is reported in dimensionless units $T^* = Tk_B/\epsilon$.) Note that the bulk melting temperature for the corresponding pure system is approximately $T_m^* = 0.71$. By selecting the temperature in a suitable range and slowly changing α in the equilibration stages particle evaporation can be made a rare event. The relevant temperature range is small since T^* must be sufficiently large that the cluster is liquidlike but not so large that extensive evaporation occurs.

Over the entire range of α values studied, $\alpha = 0.9-0.3$, phase separation occurred; indeed, it appears that the mixed clusters will segregate for all values of α significantly less than unity under our simulation conditions. The average separation between the centers of mass of species A and B, $\langle d \rangle$, where $d \equiv |\mathbf{d}| = |\mathbf{R}_A - \mathbf{R}_B|$ with

TABLE I. Cluster properties versus α for $N = 110$.

α	$\langle T^* \rangle$	$\langle R_1 \rangle$	$\langle R_2 \rangle$	$\langle R_3 \rangle$	$\langle d \rangle$
1.0	0.34	2.01	1.94	1.84	0.40
0.9	0.34	2.02	1.95	1.85	1.15
0.8	0.33	2.04	1.97	1.82	2.36
0.7	0.34	2.12	2.04	1.77	2.74
0.6	0.32	2.19	2.13	1.70	3.04
0.5	0.32	2.27	2.21	1.66	3.29
0.4	0.32	2.34	2.28	1.64	3.49
0.3	0.32	2.50	2.45	1.59	3.89

$\mathbf{R}_\beta = N_\beta^{-1} \sum_{i=1}^{N_\beta} \mathbf{r}_i^{(\beta)}$, and the average principal radii of gyration of the cluster, $\langle R_1 \rangle$, $\langle R_2 \rangle$, and $\langle R_3 \rangle$, can be used to characterize the gross features of the binary cluster. Here the angle brackets denote time averages for the MD simulations and averages over the Markov chain for the MC simulations. Table I presents data for $N = 110$ obtained using constant energy MD. The results show a rapid increase in $\langle d \rangle$ followed by a slower increase with decreasing α. These trends are similar for all values of N studied. Figure 1 shows sample configurations corresponding to three values of α for $N = 110$ obtained from constant energy MD simulations. The change in overall shape of the phase-separated cluster is evident in the configurations in Fig. 1 and is reflected in the principal radii of gyration. The interfacial area between the two subclusters decreases as α decreases. This effect is a function of temperature.

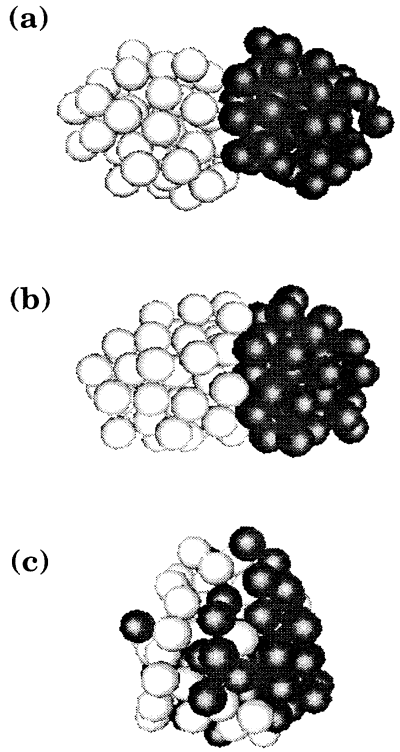

FIG. 1. Phase-separated configurations for (a) $\alpha = 0.3$, (b) $\alpha = 0.5$, and (c) $\alpha = 0.9$ showing the elongation of the cluster and increase of interfacial area as α increases. The average temperatures corresponding to these configurations are given in Table I.

There is strong structural ordering within the subclusters. To investigate this order it is useful to consider a cylindrical coordinate system with the z axis along the instantaneous vector $\mathbf{d}$ joining the centers of mass of the two species, with the z origin at the center of mass of the binary cluster. Here the particle density, $\rho_\beta(z)$, is defined as the average number of β-type particles per volume contained within a cylindrical slab of radius 2σ and thickness dz, normalized so that $\int dz\, \rho_\beta = 1$. The particle densities exhibit prominent oscillations as a function of z (cf. Fig. 2). The figure shows that there is little penetration of one phase into the other and the separation between maxima is approximately σ: each subcluster acts as a "wall" for its mate and is responsible for inducing strong particle density correlations akin to those observed in fluids next to solid surfaces. The correlations persist throughout the cluster, even for quite large clusters up to $N = 240$. These cluster density profiles differ from those of the liquid-liquid interface separating two bulk phases, where far less structure is observed [10]. In spite of these strong density correlations the clusters are liquidlike under the conditions of the simulation. The picture of the static structure that emerges from this study is that of two droplets or subclusters "welded" to each other with each subcluster inducing strong particle density correlations within the other. Of course, there is structural ordering in pure clusters but this ordering is radial in character and is different from that arising from the presence of an interface between the two liquid regions. Thus, the internal structure of these binary liquid clusters is quite different from either bulk liquid or the liquid phases of pure clusters.

Cooling of such phase-separated clusters can produce interesting solid structures. It is now well established [4,11] that the $T = 0$ ground state configurations of pure

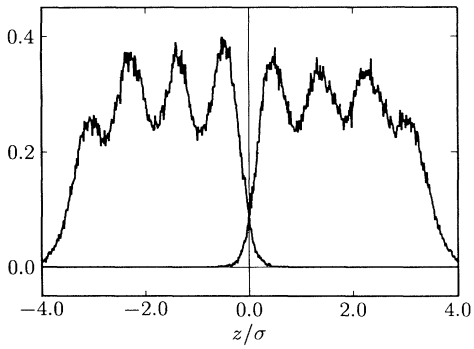

FIG. 2. Average densities $\rho_A(z)$ and $\rho_B(z)$ along z as a function of z/σ for an $N = 110$ cluster with $\alpha = 0.5$ at $T^* = 0.32$ obtained from a constant energy MD simulation. Each $\rho_\beta(z)$ is normalized to have unit area.

LJ clusters are icosahedral structures for all cluster sizes up to about $N = 5000$. This is the case for free clusters. However, since phase-separated binary liquid clusters are strongly ordered about the interface, it seems reasonable to ask if this order causes the clusters to solidify into a different structure. We find that this is definitely not the case; the ground state configurations of the binary clusters are icosahedral [12]. For example, a cluster with 27 A atoms and 28 B atoms with $\alpha = 0.5$ forms a slightly distorted 55 atom Mackay icosahedral cluster. Similarly, a binary cluster with $\alpha = 0.5$ and $N = 76$ forms a distorted 55 atom Mackay icosahedral cluster with a 21 atom appendage; this appendage also has icosahedral order.

Phase separation dynamics.—The phase separation dynamics of a binary mixture composed of two partially miscible components involves a complex interplay between interfacial and bulk properties [13]. Following a quench from the mixed state to the two-phase region, the evolution proceeds through domain formation and coarsening processes. The description of both the early and late stages of the evolution presents theoretical challenges: the early stage is complicated by the fact that well-defined structures have not yet formed and the system is highly sensitive to molecular fluctuations. Although fluctuations are less important and macroscopic descriptions retain their utility in the late-stage dynamics, domain coarsening is difficult to describe since the order parameter dynamics couples to the bulk hydrodynamic modes, due to the existence of a conservation law.

In a bulk binary fluid a critical quench is carried out by taking a system in the one-phase region at the critical composition and suddenly changing a thermodynamic variable such as the temperature to a value in the two-phase region. In clusters we are dealing with metastable states and there are various ways one can imagine preparing mixed or partially mixed binary clusters under different nonequilibrium conditions. As a result, in order to investigate the phenomenology of demixing, we examine evolution from initial nonequilibrium states constructed in the following way: After equilibrating the cluster for $\alpha = 1$, the velocities are selected from a Maxwell distribution with a given temperature T and α is changed to a prescribed value less than unity. The subsequent evolution is followed by constant energy MD. The initial temperature must be selected to be sufficiently small to make evaporation a rare event on the time scale of the phase separation process. Different realizations of the phase separation dynamics are obtained by selecting different random positions for the two species in the mixed cluster and different initial velocities.

The local concentration is not a convenient order parameter for small anisotropic clusters. In its place we use $\phi(t) = d(t) - d_0$, where $d(t)$ is the instantaneous separation between the centers of mass of the two components and $d_0 \approx \sigma$ is the average value of $\langle d \rangle$ for a fully mixed cluster ($\alpha = 1$). The quantity d_0 is approximately σ in the mixed state as a result of particle exclusion effects.

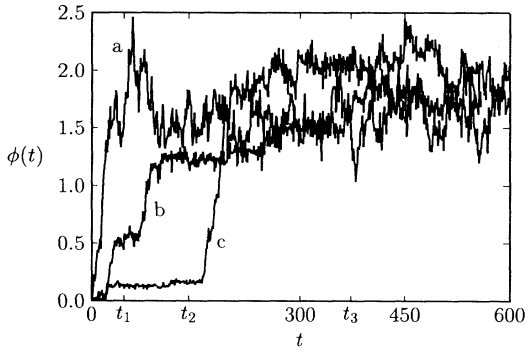

FIG. 3. Constant energy MD results for $\phi(t)$ versus t [in units of $\tau = (m\sigma^2/\epsilon)^{1/2}$] for three realizations of the phase separation process for an $N = 50$ cluster with $\alpha = 0.5$.

Thus, $\langle \phi(t) \rangle$ varies from zero in the mixed state to some finite value in the phase-separated state and provides a rough way to monitor the phase separation dynamics. The plots of $\phi(t)$ versus the time t in Fig. 3 show that phase separation can occur by different routes depending on the realization of the process: For $N = 50$ most realizations show a smooth increase of $\phi(t)$ as in (a) while in other cases, (b) and (c), $\phi(t)$ evolves to its asymp-

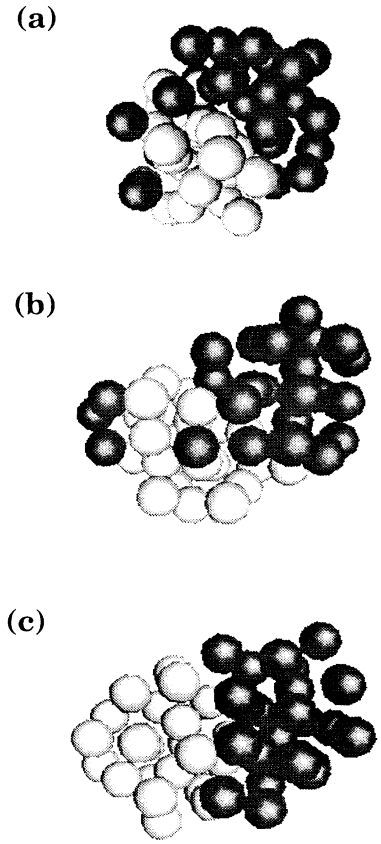

FIG. 4. Configurations corresponding to the steps in the evolution of $\phi(t)$ in curve b of Fig. 3 at times t_1, t_2, and t_3.

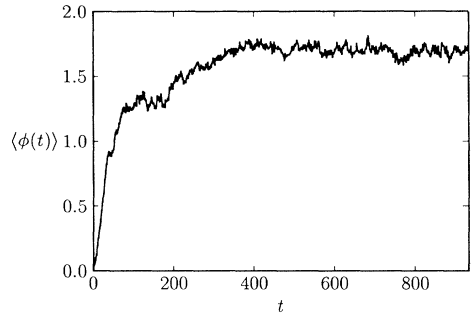

FIG. 5. Average of $\phi(t)$, $\langle\phi(t)\rangle$, over twenty realizations of the phase separation process versus t (in units of τ) for clusters with $N = 50$ and $\alpha = 0.5$.

totic value through a series of steplike jumps. Steplike regions with low values of $\phi(t)$ can be associated with an initial demixing process leading to the formation of microdomains, or in some cases directly to the fully demixed state. The steplike regions with higher values of $\phi(t)$ correspond to states in which microclusters of the individual phases exist; this stage is followed by fusion of the microclusters. This process is shown in Fig. 4 for one realization of the phase separation dynamics, corresponding to curve b in Fig. 3. The three configurations were selected at times in the plateau regions. The microclusters must diffuse as a unit before further demixing occurs and the time scale for this process can be quite long. Thus, the cluster phase separation dynamics shows incipient domain formation analogous to the early-stage dynamics, and microcluster fusion, analogous to late-stage domain coarsening in bulk binary fluids. Of course, there is a wide spread in the dynamics of individual realizations ranging from direct phase separation to phase separation governed by microcluster diffusion, as can be seen in Fig. 3. The evolution of the average order parameter $\langle\phi(t)\rangle$ is given in Fig. 5. This average over twenty realizations of the evolution process still displays step structure and indicates that phase separation is complete after about 400τ, where τ is given by $\tau = (m\sigma^2/\epsilon)^{1/2} \simeq 2.1$ ps.

While there is evidence of incipient domain formation and growth in nanoclusters, these processes are highly restricted due to the small sizes of the clusters. In addition, domain curvature and its coupling to conserved modes, which determine the late-stage dynamics in the infinite system, are difficult to define in the cluster environment. Thus, although the phase separation process proceeds through stages that mimic those in the bulk, microscopic domain sizes, the lack of well-defined macroscopic fields and strong molecular fluctuations make the quantitative description of cluster phase separation a challenging problem. Other features may also complicate the demixing process: solid and liquid phases can coexist within the subclusters that form and the number of atoms in the initial mixed cluster or subclusters can correspond to magic numbers. Both of these factors can influence the structure and dynamics. Solid-liquid coexistence can certainly change the time scale and mechanism of the demixing while the appearance of magic numbers during the course of the evolution can give rise to additional spatial correlations.

The financial support of the Natural Sciences and Engineering Research Council of Canada, and of the Network of Centres of Excellence Programme in association with the Natural Sciences and Engineering Research Council of Canada, is gratefully acknowledged.

[1] H. Reiss, P. Mirabel, and R.L. Whetten, J. Chem. Phys. **29**, 7214 (1988).
[2] R.S. Berry, T.L. Beck, H.I. Davis, and J. Jellinek, Adv. Chem. Phys. **70**, 75 (1988).
[3] H.-P. Cheng, X. Li, R.L. Whetten, and R.S. Berry, Phys. Rev. A **46**, 791 (1992).
[4] J.D. Honeycutt and H.C. Andersen, J. Phys. Chem. **91**, 4950 (1987).
[5] M.Y. Hahn and R.L. Whetten, Phys. Rev. Lett. **61**, 1190 (1988).
[6] M.E. Fisher and V. Privman, Phys. Rev. B **32**, 447 (1985).
[7] T.L. Hill, *Thermodynamics of Small Systems* (Benjamin, New York, 1963).
[8] S. Nosé, Mol. Phys. **52**, 255 (1984).
[9] D.J. McGinty, J. Chem. Phys. **58**, 4733 (1973); J.K. Lee, J.A. Barker, and F.F. Abraham, *ibid.* **58**, 3166 (1973); C.L. Briant and JJ. Burton, Nature (London) **243**, 100 (1973).
[10] M. Hayoun, M. Meyer, M. Mareschal, G. Ciccotti, and P. Turq, in *Chemical Reactivity in Liquids*, edited by M. Moreau and P. Turq (Plenum, New York, 1988), p.279.
[11] B.W. van de Waal, J. Chem. Phys. **90**, 3407 (1989).
[12] We established that the structures are icosahedral by computer graphics visualization.
[13] J.D. Gunton, M. San Miguel, and P.S. Sahni, in *Phase Transitions and Critical Phenomena*, edited by C. Domb and J.L. Lebowitz (Academic, New York, 1983), Vol. 8.